Air-Gap Flux Splitting for the Time-Harmonic Finite-Element Simulation of Single-Phase Induction Machines

Herbert De Gersem and Kay Hameyer

***Abstract*—A time-harmonic finite-element formulation is strongly coupled to fast Fourier transforms, discretising a particular kind of interface conditions. The approach enables the splitting of the elliptical air-gap field, typical for single-phase induction machines, into two contra-rotating parts that are applied to two distinct rotor models. Motional eddy-current effects can then be incorporated by slip transformation. The simulation of a capacitor-run motor demonstrates the coupled discretization scheme and the high efficiency of this approach.**

***Index Terms*—Eddy currents, finite-element methods, moving bodies, single-phase induction machines.**

I. Introduction

SINGLE-PHASE (1-ph) induction machines (IMs) mainly operate in domestic applications, e.g., fans and lawn movers [1]. Because of the increased interest in efficient operation of electrical machines, improved designs and, hence, also fast and accurate simulation techniques are required. In contrast to the case of three-phase (3-ph) IMs, simple time-harmonic (TH) finite-element (FE) solvers do not apply here. This paper extends the TH FE method by the newly developed air-gap flux-splitting approach in order to simulate 1-ph IMs as well.

II. Three-Phase Induction Machines

A fast and sufficiently accurate simulation of 3-ph IMs at steady-state is offered by TH magnetodynamic FE simulation [2]. A necessary assumption thereby is that the magnetic field in the air gap can be considered as a rotating wave

$$A_z(r_a, \theta, t) = \mathrm{Re}\left\{\underline{c}_{(1)}\sqrt{2}e^{\jmath(\omega t - \lambda\theta)}\right\}. \tag{1}$$

Here, A_z denotes the z component of the magnetic vector potential, r_a is the radius of a circle in the air gap, θ is the tangential coordinate along the circle, $\underline{c}_{(1)}$ is an effective phasor, ω is the electrical pulsation, and λ is the pole pair number [3]; underlining indicates effective phasors. The two-dimensional TH formulation is

$$-\frac{\partial}{\partial x}\left(\nu\frac{\partial \underline{A}_z}{\partial x}\right) - \frac{\partial}{\partial y}\left(\nu\frac{\partial \underline{A}_z}{\partial y}\right) + \jmath\omega s\sigma\underline{A}_z = \frac{\sigma}{\ell_z}\Delta\underline{V} \tag{2}$$

with ν the reluctivity, σ the conductivity, ℓ_z the length of the model, and $\Delta\underline{V}$ the phasor of the voltage drop between front and rear ends of the model. Motional eddy-current effects are exactly resolved by the introduction of the *slip* s defined as the relative difference between the angular speed of the rotating air-gap wave ω/λ and the mechanical speed ω_m of the rotor

$$s = \frac{\omega - \lambda\omega_m}{\omega}. \tag{3}$$

Discretising (2) on the cross section Ω of the device by n FEs $N_i(x, y)$, yields the system of equations $K\underline{u} = \underline{f}$ with

$$K_{ij} = \int_\Omega (\nu\nabla N_i \cdot \nabla N_j + \jmath\omega s\sigma N_i N_j)\,\mathrm{d}\Omega \tag{4}$$

$$\underline{f}_i = \int_\Omega \frac{\sigma}{\ell_z}\Delta\underline{V}N_i\,\mathrm{d}\Omega. \tag{5}$$

This approach for motional eddy-current simulation is called *slip transformation* and is also reliable for technical 3-ph IMs for which the assumption on the air-gap field applies only approximately [3]. If the formulation is further equipped with a nonlinear loop to account for ferromagnetic saturation and an external circuit to model the supply and the end-winding and end-ring impedances, a fast and remarkably accurate design tool for 3-ph IMs is obtained [4].

III. Single-Phase Induction Machines

A 1-ph winding fed by an alternating current generates an alternating field in the air gap. If an auxiliary winding is constructed in the quadrature axis and fed by an alternating current with another phase, an elliptical field is achieved. Because this field is principally alternating instead of rotating, slip transformation is no longer applicable. Hence, simulating 1-ph IMs requires a transient FE solver [5] or a combination of parameter extraction and equivalent circuits [6]. Both are troublesome, the former because of excessive computation times, the latter because of difficulties in considering local effects such as ferromagnetic saturation. In the special case of solid-rotor 1-ph IMs, a stationary motional FE formulation is applicable [3]. Geometrical homogenization enables this approach to devices with slotted rotor geometries as well, but is insufficiently accurate for

Manuscript received July 5, 2001. This work was supported in part by the Belgian "Fonds voor Wetenschappelijk Onderzoek Vlaanderen" under Grant G.0427.98 and in part by the Belgian Ministry of Scientific Research under Grant IUAP no. P4/20.

H. De Gersem was with the Katholieke Universiteit Leuven, Department ESAT, Division ELEN. He is now with the FB 18 Elektrotechnik und Informationstechnik, Fachgebiet Theorie Elektromagnetischer Felder, Technische Universität Darmstadt, D-64289 Darmstadt, Germany (e-mail: degersem@temf.de).

K. Hameyer is with the Katholieke Universiteit Leuven, Department ESAT, Division ELEN, B-3001 Leuven-Heverlee, Belgium (e-mail: kay.hameyer@esat.kuleuven.ac.be).

Publisher Item Identifier S 0018-9464(02)02349-X.

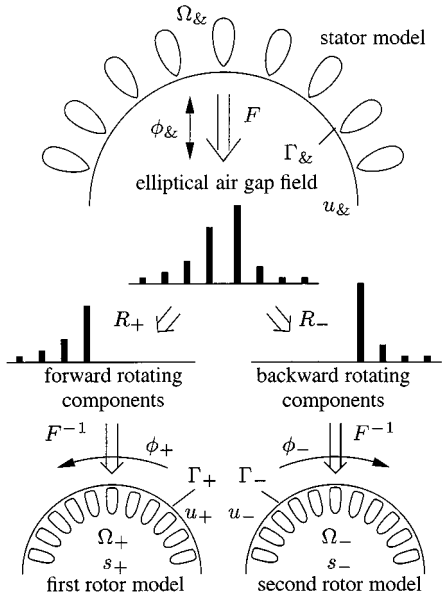

Fig. 1. Scheme of the air-gap flux-splitting approach.

technical devices [7]. The indicated inconveniences and former satisfactory results for the 3-ph case [4] motivate the development of a similar TH FE method for slotted 1-ph IMs.

IV. Air-Gap Flux Splitting

Analytical approaches for 1-ph IMs decompose the elliptical air-gap field into two contra-rotating fields, corresponding to two fictitious 3-ph IMs

$$A_z(r_a, \theta, t) = \mathrm{Re}\left\{\underline{c}_{(1)}\sqrt{2}e^{j(\omega t-\lambda\theta)} + \underline{c}_{(-1)}\sqrt{2}e^{j(\omega t+\lambda\theta)}\right\} \quad (6)$$

with $\underline{c}_{(1)}$ and $\underline{c}_{(-1)}$ the effective phasors of the forward and backward rotating components [1]. The electromotive force and the torque follow by the superposition of the 3-ph IM characteristics. The air-gap flux-splitting approach, presented here, transfers this idea into the TH FE framework. The method has the nature of a superposition technique. The elliptical air-gap flux $\phi_\&$ is split into two rotating flux components ϕ_+ and ϕ_- which are then applied to two distinct rotor models Ω_+ and Ω_- (Fig. 1). In a postprocessing step, the true solution is restored by superposing both field contributions. The splitting is required to allow a different slip value to each of the rotor models. Unfortunately, the proposed splitting of the air-gap field is not so obvious within the FE context.

The radius of the inner boundary $\Gamma_\&$ of the stator model and the outer boundaries Γ_+ and Γ_- of the rotor models is r_a. To simplify explanation and notation, an identical equidistant grid of m grid points is considered at $\Gamma_\&$, Γ_+, and Γ_-. The elliptical air-gap field at $\Gamma_\&$ is transformed into complex Fourier components $\underline{c}_\&$. In a discrete setting, this corresponds to

$$\underline{c}_\& = F\underline{u}_\& \quad (7)$$

with $\underline{u}_{\&,j}$ the FE degrees of freedom (DOFs) at $\Gamma_\&$ and F the discrete Fourier transform. If the air-gap field is pure elliptic, only the components $\underline{c}_{(1)}$ and $\underline{c}_{(-1)}$ of $\underline{c}_\&$ are nonzero, as indicated in (6). If the air-gap field is pure alternating, the magnitudes of $\underline{c}_{(1)}$ and $\underline{c}_{(-1)}$ are equal. In general, however, $\underline{c}_\&$ may contain m nonzero components $\underline{c}_{(k)}$ due to stator and rotor slotting and due to the spatial distribution of the windings.

The air-gap flux-splitting approach consists of splitting the vector $\underline{c}_\&$ in the forward- and backward-rotating component vectors $\underline{c}_+$ and $\underline{c}_-$, respectively (Fig. 1)

$$\underline{c}_+ = R_+\underline{c}_\& \quad (8)$$

$$\underline{c}_- = R_-\underline{c}_\&. \quad (9)$$

R_+ and R_- are square diagonal matrices such that $R_+ + R_- = I$. At Γ_+ and Γ_-, the decomposed air-gap fields represented by $\underline{c}_+$ and $\underline{c}_-$ are transformed into the FE DOFs $\underline{u}_+$ and $\underline{u}_-$ at Γ_+ and Γ_- by inverse discrete Fourier transformations F^{-1}

$$\underline{u}_+ = F^{-1}\underline{c}_+ \quad (10)$$

$$\underline{u}_- = F^{-1}\underline{c}_-. \quad (11)$$

Similarly, for the 3-ph IM case, motional eddy-current effects related to higher harmonics, i.e., $|k| > 1$, are neglected. For both rotor models, the slip is determined with respect to the fundamental field wave, $k = 1$ and $k = -1$, only

$$s = s_+ = \frac{\omega - \lambda\omega_m}{\omega} \quad \text{in} \quad \Omega_+ \quad (12)$$

$$s = s_- = \frac{\omega + \lambda\omega_m}{\omega} \quad \text{in} \quad \Omega_-. \quad (13)$$

This approach allows to consider the motional eddy currents due to the fundamental forward and backward flux components without time-stepping and moving meshes. The important influence of the third harmonics could be considered by two additional rotor models, which is not done here. For numerical efficiency, it is recommended to couple the splitting relations (7)–(10) together with the FE formulation in one system of equations.

V. Variational Formulation

Because of (7)–(10), the FE coefficients contained in $\underline{u}_\&$, $\underline{u}_+$ and $\underline{u}_-$ are not independent. A variational approach, however, requires a set of independent DOFs associated to a set of independent trail and test functions. Therefore, the rotor boundaries Γ_+ and Γ_- are treated as *slave* boundaries, both referring to the same *master* boundary $\Gamma_\&$. The unknowns at Γ_+ and Γ_- are related to those at $\Gamma_\&$ by

$$\underbrace{\begin{bmatrix}\underline{u}_o\\ \underline{u}_\&\\ \underline{u}_+\\ \underline{u}_-\end{bmatrix}}_{\underline{u}} = \underbrace{\begin{bmatrix}I & 0\\ 0 & I\\ 0 & F^{-1}R_+F\\ 0 & F^{-1}R_-F\end{bmatrix}}_{P} \underbrace{\begin{bmatrix}\underline{u}_o\\ \underline{u}_\&\end{bmatrix}}_{\underline{w}} \quad (14)$$

with $\underline{u}_o$ the DOFs inside the stator and rotor models. It is also possible to consider the Fourier coefficients as the independent unknowns

$$\underbrace{\begin{bmatrix}\underline{u}_o\\ \underline{u}_{\&}\\ \underline{u}_+\\ \underline{u}_-\end{bmatrix}}_{\underline{u}} = \underbrace{\begin{bmatrix}I & 0\\ 0 & F^{-1}\\ 0 & F^{-1}R_+\\ 0 & F^{-1}R_-\end{bmatrix}}_{P} \underbrace{\begin{bmatrix}\underline{u}_o\\ \underline{c}_{\&}\end{bmatrix}}_{\underline{w}}. \tag{15}$$

In both cases, the overall set of unknowns $\underline{w}$ corresponds to an independent set of shape functions. Hence, a variational approach can be applied, resulting in the system of equations

$$P^H K P \underline{w} = P^H \underline{f}. \tag{16}$$

P^H contains the operators F^{-H}, R_+^H, and R_-^H which are equal to F, R_+, and R_-, respectively.

The variational formulation explicitly eliminates the FE unknowns at the slave boundaries with respect to unknowns at the master boundary. Hence, all unknowns represent independent DOFs and the existence and uniqueness of a solution to the problem is easily checked. The formulation explicitly constructs the FE spaces that invoke the splitting and guarantees the continuity requirements for both the normal component of the magnetic flux density and the tangential component of the magnetic field strength in the air-gap area. This approach has particular disadvantages. The supports of the shape functions associated with $\underline{u}_{\&}$ or $\underline{c}_{\&}$ are considerably larger compared with those of common FE shape functions. This is reflected in the system matrix $P^H K P$ by an $m \times m$ dense block introduced by the Fourier transforms. The explicit construction of $P^H K P$ is therefore strongly discouraged. Instead, only K is built. P and P^H are applied as operators. Hence, the system matrix $P^H K P$ only exists in factorized form. This is sufficient for Krylov subspace system solvers since these only need matrix–vector multiplications. If the grids at $\Gamma_{\&}$, Γ_+, and Γ_- are equidistant and matching, fast Fourier transforms (FFT) and inverse FFTs allow the most efficient application of F and F^{-1}.

VI. Saddle-Point Formulation

An alternative formulation maintains the vectors of unknowns $\underline{u}_+$ and $\underline{u}_-$ as unknowns in the formulation. The FE system of equations $K\underline{u} = \underline{f}$ corresponds to the situation as if homogeneous Neumann constraints were applied at $\Gamma_{\&}$, Γ_+, and Γ_-. The unknown magnetic field strength along the edges of $\Gamma_{\&}$, Γ_+, and Γ_- are collected in $\underline{g}_{\&}$, $\underline{g}_+$, and $\underline{g}_-$ and expressed by

$$\begin{bmatrix}0\\ \underline{g}_{\&}\\ \underline{g}_+\\ \underline{g}_-\end{bmatrix} = \underbrace{\begin{bmatrix}0 & 0\\ F^{-1}R_+ & F^{-1}R_-\\ -F^{-1} & 0\\ 0 & -F^{-1}\end{bmatrix}}_{B^H} \underbrace{\begin{bmatrix}\underline{\psi}\\ \underline{\xi}\end{bmatrix}}_{\underline{p}} \tag{17}$$

with $\underline{\psi}$ and $\underline{\xi}$ two $m \times 1$-vectors. Notice that (17) explicitly implies the necessary continuity relation for the magnetic field strength: $\underline{g}_{\&} + \underline{g}_+ + \underline{g}_- = 0$. The continuity and splitting of the magnetic flux density in the air gap is enforced by the additional constraints

$$\underbrace{\begin{bmatrix}0 & R_+F & -F & 0\\ 0 & R_-F & 0 & -F\end{bmatrix}}_{B} \underbrace{\begin{bmatrix}\underline{u}_o\\ \underline{u}_{\&}\\ \underline{u}_+\\ \underline{u}_-\end{bmatrix}}_{\underline{u}} = \begin{bmatrix}0\\ 0\end{bmatrix}. \tag{18}$$

Equations (17) and (18) constitute a *saddle-point* problem

$$\begin{bmatrix}K & B^H\\ B & 0\end{bmatrix}\begin{bmatrix}\underline{u}\\ \underline{p}\end{bmatrix} = \begin{bmatrix}\underline{f}\\ 0\end{bmatrix}. \tag{19}$$

The vectors $\underline{\psi}$ and $\underline{\xi}$ can be interpreted as two sets of Lagrange multipliers [8]. B has size $2m \times n$ and is of full rank. K is an $n \times n$ matrix and consists of three diagonal blocks corresponding to 1 stator and 2 rotor models. Since the rotor models have only Neumann constraints, a solution $\underline{a}$ of $K\underline{a} = \underline{b}$ for a given right-hand side $\underline{b}$ is only defined up to one additive constant per rotor model. As a consequence, K has rank $n-2$. The existence and uniqueness of a solution of (19) is guaranteed by the properties of the discrete Fourier transforms embedded in B [8].

$\hat{K}$ denotes an operator equivalent to K, i.e., $\hat{K}\underline{a} = K\underline{a} = \underline{b}$ for $\underline{b} \in \mathrm{Ran}K$, and incorporating one additional constraint per rotor model. It is now possible to eliminate the vector of unknowns $\underline{u}$ from (19) and solve the reduced system

$$\underbrace{B\hat{K}^{-1}B^H}_{S}\underline{p} = B\hat{K}^{-1}\underline{f}. \tag{20}$$

This approach is however not rewarding in practice. The computation of the matrix S requires the computation of $\hat{K}^{-1}B^H$ which is too expensive. Instead, preconditioned Krylov-type methods, directly applied to the mixed formulation (19), are favored. Due to the off-diagonal blocks B and B^H, the saddle-point problem (19) does not preserve the complex symmetry of the FE matrix part K. Hence, Krylov subspace solvers for nonsymmetric systems, such as Biconjugate Gradients Stabilized and Generalized Minimal Residual, are due.

VII. Benchmark Model

The air-gap flux-splitting approach is tested for a simple solid-rotor 1-ph IM (Fig. 2). The stator excitation is replaced by an alternating- or elliptical-field boundary condition at the outer radius of the model. The air gap is not shown in the figures. The magnetic flux lines are plotted for two instants of time, t_0 and t_1, a quarter of a period shifted in time. The true solution is shown on the rotor within the stator. The fields in the left and right rotor models at t_0 and t_1 feature the same flux patterns shifted over 90° mechanically, indicating their rotating nature. For a locked rotor excited by an alternating field, $s_+ = s_-$, and both rotor models behave similarly, yielding a symmetric, alternating, overall field. In the situation of the locked rotor excited by an elliptical field, $s_+ \neq s_-$, both flux patterns differ and constitute a nonsymmetric air-gap field. In the case of rotor

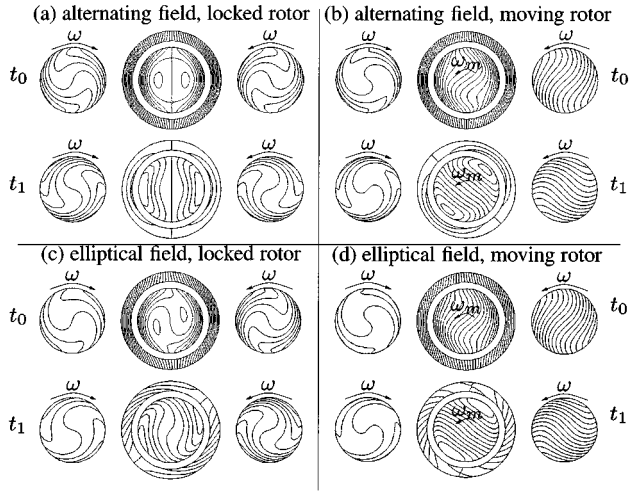

Fig. 2. Solid-rotor 1-ph IM model: Magnetic flux line plots at t_0 and t_1 for a locked (left) and a moving (right) rotor excited by an alternating (above) or elliptical (below) field.

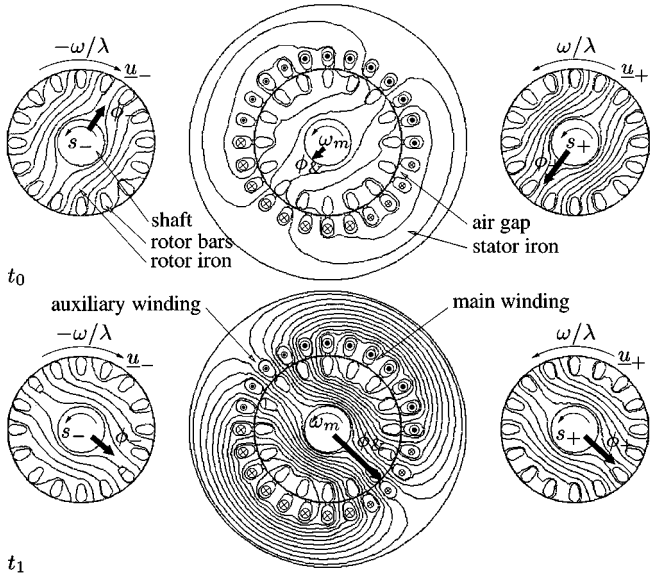

Fig. 3. Plot of the magnetic flux lines at t_0 and t_1 of the start/run-capacitor motor model operating at slip 0.5.

movement, $s_+ \neq s_-$, and different flux patterns are observed for both the alternating and elliptical air-gap field.

VIII. Application

The FE flux-splitting approach is applied to simulate a loaded capacitor-run 1-ph IM. Both stator and rotor are slotted. The alternating field excited by the main winding is augmented by a field generated by an auxiliary winding, put in the quadrature axis of the main one and series connected to a capacitor. End-effects and the electrical supply are modelled by an external circuit coupled to the FE model [9]. The ferromagnetic saturation of the stator and rotor iron is taken into account by subsuccessive substitution [9]

The magnetic flux lines for the slips $s_+ = 0.5$ and $s_- = 1.5$ are plotted in Fig. 3. The middle rotor model serves for superposing the solutions, evaluating the nonlinear characteristic of the ferromagnetic iron and visualizing the final solution. The magnitude of the fundamental backward rotating wave is 38% compared with the magnitude of the fundamental forward rotating wave. Hence, the reverse torque component cannot be neglected. The higher order components, $|k| > 1$, are less important because they generate currents and torques which scale as $1/k$ and $1/k^2$, respectively. The method enables the computation of the torque, the eddy currents, and the local losses at a steady-state with a certain speed, up to the technically required accuracy, within a single computational step. The same method applies without modifications to shaded-pole IMs and reluctance-start IMs [1].

IX. Conclusion

The decomposition of the elliptical air-gap flux of a capacitor motor model allows to distribute forward- and backward-rotating components to two distinct rotor models. Motional eddy currents are efficiently taken into account by slip transformation. The coupled TH FE formulation with air-gap flux splitting results in a fast simulation tool for steady-state operations of rotating single-phase IMs.

Acknowledgment

The authors would like to thank ATB Austria for providing the material data of the capacitor-run motor.

References

[1] C. G. Veinott, *Fractional- and Subfractional-Horsepower Electric Motors*, 3rd ed. New York: McGraw-Hill, 1970.

[2] E. Vassent, G. Meunier, and J. C. Sabonnadière, "Simulation of induction machine operation using complex magnetodynamic finite elements," *IEEE Trans. Magn.*, vol. 25, pp. 3064–3066, July 1989.

[3] H. De Gersem, R. Mertens, and K. Hameyer, "Comparison of time-harmonic and transient finite element models for asynchronous machines," in *Proc. Int. Conf. Electrical Machines (ICEM00)*, vol. 1, Helsinki, Finland, pp. 66–70.

[4] R. De Weerdt, E. Tuinman, K. Hameyer, and R. Belmans, "Finite element analysis of steady-state behavior of squirrel cage induction motors compared with measurements," *IEEE Trans. Magn.*, vol. 33, pp. 2093–2096, Mar. 1997.

[5] N. Sadowski, R. Carlson, S. R. Arruda, C. A. da Silva, and M. Lajoie-Mazenc, "Simulation of single-phase induction motor by a general method coupling field and circuit equations," *IEEE Trans. Magn.*, vol. 31, pp. 1908–1911, May 1995.

[6] S. Williamson and A. C. Smith, "A unified approach to the analysis of single-phase induction motors," *IEEE Trans. Ind. Applicat.*, vol. 35, pp. 837–843, July 1999.

[7] H. De Gersem and K. Hameyer, "Finite element simulation of motional eddy currents in slotted geometries," *JSAEM Studies Appl. Electromagn. Mech.*, submitted for publication.

[8] F. Brezzi and M. Fortin, *Mixed and Hybrid Finite Element Methods*. Berlin, Germany: Springer-Verlag, 1991.

[9] H. De Gersem, K. Debrabandere, R. Belmans, and K. Hameyer, "Motional time-harmonic simulation of slotted single-phase induction machines," *IEEE Trans. Energy Conversion*, submitted for publication.